

CrossMark  
click for updates

# An 80.11% FF record achieved for perovskite solar cells by using the NH<sub>4</sub>Cl additive†

Cite this: *Nanoscale*, 2014, 6, 9935

Chuantian Zuo and Liming Ding\*

Received 5th May 2014  
Accepted 3rd July 2014

DOI: 10.1039/c4nr02425g

www.rsc.org/nanoscale

The light-absorbing perovskite layer fabricated using the NH<sub>4</sub>Cl additive shows high crystallinity and better morphology. The resulting solar cells gave a decent power conversion efficiency of 9.93% and a fill factor record of 80.11%. This work provides a very simple but effective approach to enhance the power conversion efficiency of perovskite solar cells.

Perovskite solar cells using organometal halide perovskites as light-absorbing materials have received a great deal of attention due to their excellent photovoltaic performance.<sup>1–4</sup> CH<sub>3</sub>NH<sub>3</sub>PbX<sub>3</sub> (X = Br, I) perovskite nanocrystals were used as sensitizers in dye-sensitized solar cells (DSSCs) and a power conversion efficiency (PCE) of 3.8% was obtained in 2009.<sup>5</sup> Later, Park *et al.* reported an improved PCE of 6.54% by using CH<sub>3</sub>NH<sub>3</sub>PbI<sub>3</sub> nanocrystals in DSSCs.<sup>6</sup> In solid-state hybrid solar cells, PCEs of 10.9% and 9.7% were achieved when CH<sub>3</sub>NH<sub>3</sub>PbI<sub>2</sub>Cl and CH<sub>3</sub>NH<sub>3</sub>PbI<sub>3</sub> were used as the absorbers, respectively.<sup>1,2</sup> Recently, Wojciechowski *et al.* reported a 15.9% PCE in meso-superstructured perovskite solar cells.<sup>7</sup> Perovskites are excellent semiconductors in solar cells due to their panchromatic light absorption, ambipolar transport and very long electron/hole diffusion lengths.<sup>8,9</sup> A great deal of effort has been paid by researchers to explore this brand-new solar cell, *e.g.* developing low-temperature fabrication methods,<sup>4</sup> making new hole conductors<sup>10</sup> and trying flexible substrates.<sup>11</sup>

Perovskite solar cells with device structure indium tin oxide (ITO)/poly(3,4-ethylenedioxythiophene):polystyrene sulfonate (PEDOT:PSS)/perovskite/[6,6]-phenyl-C<sub>61</sub>-butyric acid methyl ester (PC<sub>61</sub>BM)/Al are becoming popular because they can be made into flexible devices and processed at 150 °C.<sup>11–16</sup> Malinkiewicz *et al.* sandwiched sublimated CH<sub>3</sub>NH<sub>3</sub>PbI<sub>3</sub> between the organic hole-transport layer and PC<sub>61</sub>BM, and obtained a 12% PCE.<sup>15</sup> Lam *et al.* developed solution-processed CH<sub>3</sub>NH<sub>3</sub>PbI<sub>3</sub>/

PC<sub>61</sub>BM solar cells and obtained a 5.2% PCE using a one-step deposition method and a 7.4% PCE using a sequential deposition method.<sup>13</sup> Kim *et al.* improved the morphology of the CH<sub>3</sub>NH<sub>3</sub>PbI<sub>3</sub> layer using solvent mixtures and obtained a PCE of 6.2%.<sup>16</sup> The crystallinity and morphology of perovskite layers are very important for the performance of perovskite solar cells.<sup>16,17</sup>

Here, we report an innovative approach by using chloride additives to improve the crystallinity and morphology of perovskite layers, and the performance of solar cells. The effects of CH<sub>3</sub>NH<sub>3</sub>Cl and NH<sub>4</sub>Cl additives on the crystallinity and morphology of perovskite layers were studied. The additives helped to form flawless perovskite nanocrystals and also helped to form smooth and uniform films, leading to better device performance. A solution-processed device with the structure of ITO/PEDOT:PSS/CH<sub>3</sub>NH<sub>3</sub>PbI<sub>3</sub>/PC<sub>61</sub>BM/Al was studied. The device fabricated using NH<sub>4</sub>Cl as an additive gave a PCE around 10% and a fill factor (FF) over 80%.

The structure of CH<sub>3</sub>NH<sub>3</sub>PbI<sub>3</sub>/PC<sub>61</sub>BM solar cells is shown in Fig. 1. PC<sub>61</sub>BM is often used as an electron acceptor in organic solar cells and it can effectively quench the photoluminescence of perovskites in a bi-layer structure.<sup>18</sup> So PC<sub>61</sub>BM can act as an electron acceptor and electron collection layer in perovskite



Fig. 1 Structure of CH<sub>3</sub>NH<sub>3</sub>PbI<sub>3</sub>/PC<sub>61</sub>BM solar cells.

National Center for Nanoscience and Technology, Beijing 100190, China. E-mail: opv.china@yahoo.com

† Electronic supplementary information (ESI) available: Experimental details, measurements and instruments. See DOI: 10.1039/c4nr02425g

solar cells. Under illumination, excitons generated in the perovskite layer will dissociate at the perovskite/PC<sub>61</sub>BM interface.<sup>14,18</sup> Electrons move to the LUMO of PC<sub>61</sub>BM and are collected by the Al electrode. PEDOT is used as a hole-transport layer, holes move to the PEDOT layer and are collected by the ITO electrode.

We first investigated the effect of additives on light absorption and crystallization of the CH<sub>3</sub>NH<sub>3</sub>PbI<sub>3</sub> film through UV-vis spectra and X-ray diffraction (XRD). All the films for absorption and XRD measurements were prepared under the same conditions except the difference of additives in perovskite precursor solution (in DMF). The film thickness is around 140–150 nm. As shown in Fig. 2a, all films show absorption onsets at ca. 780 nm. Films prepared using CH<sub>3</sub>NH<sub>3</sub>Cl and NH<sub>4</sub>Cl additives exhibit an absorption peak at ca. 360 nm and a shoulder at ca. 476 nm. The shape of the UV-vis spectra is similar to the reported results.<sup>13</sup> The film prepared using the NH<sub>4</sub>Cl additive shows stronger absorption at 310–500 nm than the film prepared using the CH<sub>3</sub>NH<sub>3</sub>Cl additive. The film prepared using no additive shows red shift, which might be due to the poor crystallization of CH<sub>3</sub>NH<sub>3</sub>PbI<sub>3</sub> in the thick film.<sup>19</sup> The XRD peak positions for all CH<sub>3</sub>NH<sub>3</sub>PbI<sub>3</sub> films on PEDOT:PSS coated glass substrates are nearly the same (Fig. 2b). The diffraction peaks of the CH<sub>3</sub>NH<sub>3</sub>PbI<sub>3</sub> film prepared using the NH<sub>4</sub>Cl additive at 14.28°, 28.62° and 43.42° can be assigned to (110), (220) and (330)

planes, respectively. The diffraction intensities for CH<sub>3</sub>NH<sub>3</sub>PbI<sub>3</sub> films prepared using different additives are quite different. The inset in Fig. 2b shows the peaks at 14.28°. The diffraction intensity of the CH<sub>3</sub>NH<sub>3</sub>PbI<sub>3</sub> film prepared using the NH<sub>4</sub>Cl additive is much stronger than that of the film prepared using the CH<sub>3</sub>NH<sub>3</sub>Cl additive. The diffraction peaks of the film prepared using no additive are very weak, suggesting that the additives favor CH<sub>3</sub>NH<sub>3</sub>PbI<sub>3</sub> crystallization and NH<sub>4</sub>Cl is more effective. Strong diffraction peaks for a thin CH<sub>3</sub>NH<sub>3</sub>PbI<sub>3</sub> film (150 nm) prepared using the NH<sub>4</sub>Cl additive indicate that CH<sub>3</sub>NH<sub>3</sub>PbI<sub>3</sub> is highly crystalline. The size of the nanocrystals in CH<sub>3</sub>NH<sub>3</sub>PbI<sub>3</sub> films is ca. 40 nm, which was calculated from the peak width of the XRD pattern. The XRD patterns for CH<sub>3</sub>NH<sub>3</sub>Cl and NH<sub>4</sub>Cl films can be found in Fig. S1.† The diffraction peaks of CH<sub>3</sub>NH<sub>3</sub>Cl and NH<sub>4</sub>Cl cannot be found in XRD patterns of CH<sub>3</sub>NH<sub>3</sub>PbI<sub>3</sub> films prepared using the additives, so there is no CH<sub>3</sub>NH<sub>3</sub>Cl or NH<sub>4</sub>Cl crystal in CH<sub>3</sub>NH<sub>3</sub>PbI<sub>3</sub> films. The effect of annealing time on CH<sub>3</sub>NH<sub>3</sub>PbI<sub>3</sub> crystallization was studied. The diffraction intensity for the CH<sub>3</sub>NH<sub>3</sub>PbI<sub>3</sub> film prepared using no additive does not change with annealing time (Fig. S2†). However, the diffraction intensity of the CH<sub>3</sub>NH<sub>3</sub>PbI<sub>3</sub> film prepared using the NH<sub>4</sub>Cl additive increases significantly after being annealed at 100 °C for 30 s. Then XRD patterns remain nearly unchanged, indicating that CH<sub>3</sub>NH<sub>3</sub>PbI<sub>3</sub> crystallization accomplishes (Fig. S3†).

Perovskite film morphology and surface coverage are crucial to the performance of planar heterojunction perovskite solar cells.<sup>17</sup> So we investigated the morphology of CH<sub>3</sub>NH<sub>3</sub>PbI<sub>3</sub> films prepared using different additives by scanning electron microscopy (SEM) and atomic force microscopy (AFM). CH<sub>3</sub>NH<sub>3</sub>PbI<sub>3</sub> films were prepared on PEDOT:PSS coated ITO substrates *via* spin-coating perovskite precursor solution and heating at 100 °C for 30 s. Fig. 3 shows SEM and AFM images of CH<sub>3</sub>NH<sub>3</sub>PbI<sub>3</sub> films prepared using different additives. The SEM image of the film prepared using no additive exhibited large voids and extremely rough surface. The larger scale image is shown in Fig. S4,† a fiber-like solid and voids in the film can be seen clearly. Nearly no voids can be seen in the film prepared using the CH<sub>3</sub>NH<sub>3</sub>Cl additive. Pebble-like nanocrystals (70–200 nm) are distributed in the film. The film prepared using the NH<sub>4</sub>Cl additive contains uniform nanocrystals (Fig. 3c) and shows better coverage than the film prepared using the CH<sub>3</sub>NH<sub>3</sub>Cl additive (Fig. S4†). The film prepared using no additive exhibited a root-mean-square (RMS) roughness of 47.5 nm. Films prepared using CH<sub>3</sub>NH<sub>3</sub>Cl and NH<sub>4</sub>Cl additives are much smoother, showing RMS roughnesses of 15.3 nm and 5.2 nm, respectively. The RMS roughness for the film prepared using the NH<sub>4</sub>Cl additive is even smaller than that of the best perovskite film reported previously.<sup>16</sup> AFM phase images are consistent with SEM images. Comparing the phase images of the three films, we observe that the films prepared using additives show small and uniform domains, providing a smooth perovskite surface for forming a high-quality PC<sub>61</sub>BM layer.

Solar cells with structure ITO/PEDOT:PSS/CH<sub>3</sub>NH<sub>3</sub>PbI<sub>3</sub>/PC<sub>61</sub>BM/Al were fabricated to investigate the effect of additives on photovoltaic performance. Device performance data are listed in Table 1. The device fabricated using no additive exhibited

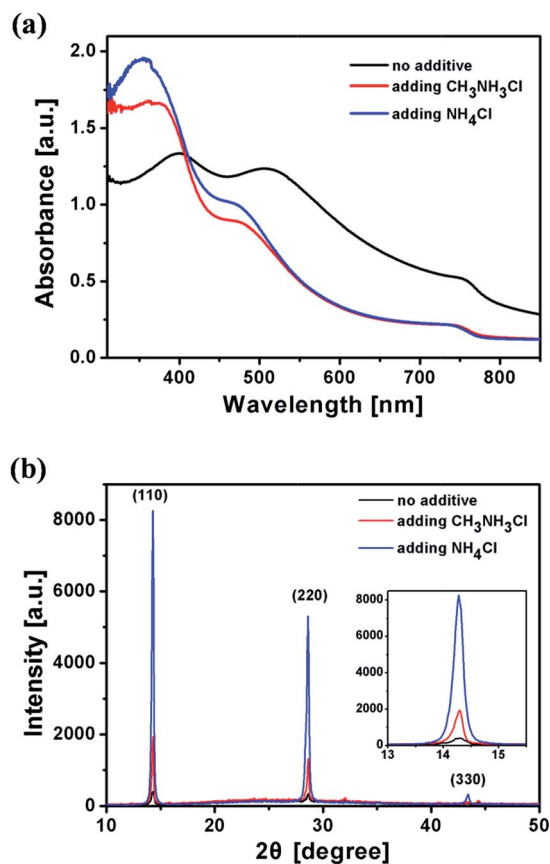


Fig. 2 UV-vis absorption spectra (a) and XRD patterns (b) for CH<sub>3</sub>NH<sub>3</sub>PbI<sub>3</sub> films fabricated by using different additives.

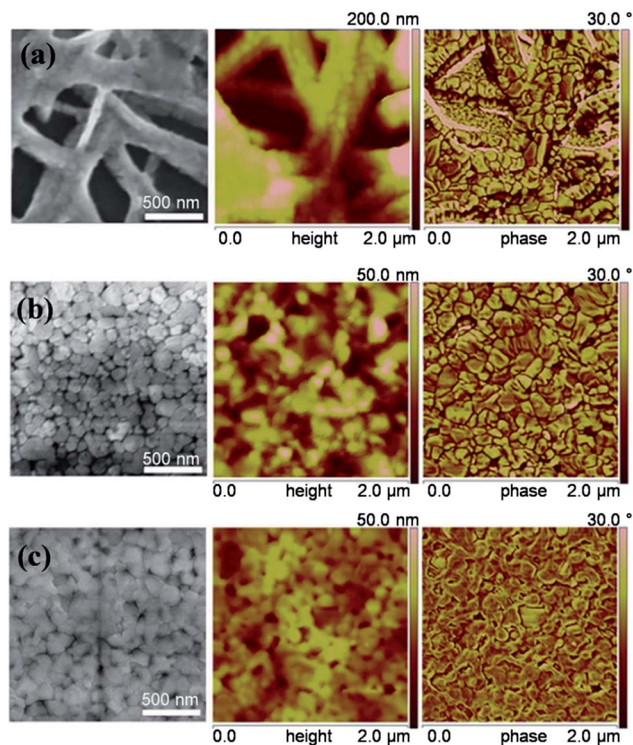


Fig. 3 SEM (left), AFM height (middle) and phase (right) images for  $\text{CH}_3\text{NH}_3\text{PbI}_3$  films fabricated using no additive (a),  $17.5 \text{ mg mL}^{-1}$   $\text{CH}_3\text{NH}_3\text{Cl}$  (b), and  $17.5 \text{ mg mL}^{-1}$   $\text{NH}_4\text{Cl}$  (c), respectively.

Table 1 Performance data for  $\text{CH}_3\text{NH}_3\text{PbI}_3$  solar cells

Additive	$V_{oc}$ [V]	$J_{sc}$ [ $\text{mA cm}^{-2}$ ]	FF [%]	PCE (average <sup>a</sup> ) [%]
Without	0.37	0.36	27.53	0.04 (0.03)
$\text{CH}_3\text{NH}_3\text{Cl}$	0.92	12.78	69.40	8.16 (7.97)
$\text{NH}_4\text{Cl}$	0.88	14.08	80.11	9.93 (9.75)

<sup>a</sup> Average PCE of 20 devices.

an open-circuit voltage ( $V_{oc}$ ) of 0.37 V, a short-circuit current density ( $J_{sc}$ ) of  $0.36 \text{ mA cm}^{-2}$ , a fill factor of 27.53% and a power conversion efficiency (PCE) of 0.04% (Fig. 4). The performance of the device fabricated using no additive being inconsistent with previous reports<sup>13,16</sup> is due to the thickness difference between  $\text{CH}_3\text{NH}_3\text{PbI}_3$  films. The  $\text{CH}_3\text{NH}_3\text{PbI}_3$  film fabricated in this work using no additive is thicker (*ca.* 150 nm), and the imperfect crystallinity and morphology lead to poor device performance. Thick  $\text{CH}_3\text{NH}_3\text{PbI}_3$  films with high crystallinity and good morphology are obtained by using additives, and they give higher  $J_{sc}$  than previous films.<sup>13,16</sup> The optimization data for device performance are listed in Tables S1–S5.† The optimized concentrations of  $\text{CH}_3\text{NH}_3\text{Cl}$  and  $\text{NH}_4\text{Cl}$  additives are  $20.0 \text{ mg mL}^{-1}$  and  $17.5 \text{ mg mL}^{-1}$ , respectively. The device fabricated using the  $\text{CH}_3\text{NH}_3\text{Cl}$  additive gave a  $V_{oc}$  of 0.92 V, a  $J_{sc}$  of  $12.78 \text{ mA cm}^{-2}$ , a FF of 69.40% and a PCE of 8.16%. The device fabricated using the  $\text{NH}_4\text{Cl}$  additive gave a  $V_{oc}$  of 0.88 V, a  $J_{sc}$  of  $14.08 \text{ mA cm}^{-2}$ , a FF of 80.11% and a PCE of 9.93%. Higher  $J_{sc}$

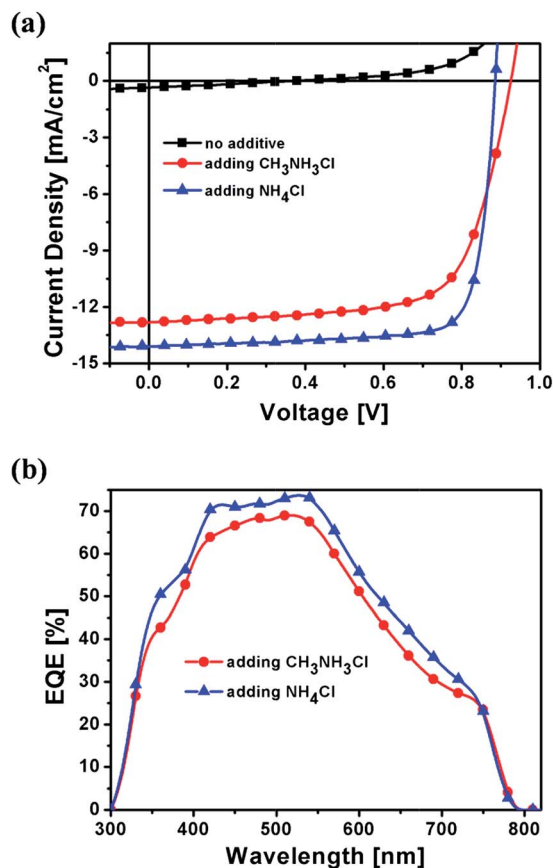


Fig. 4  $J$ - $V$  curves (a) and EQE spectra (b) for  $\text{CH}_3\text{NH}_3\text{PbI}_3$  solar cells fabricated by using different additives.

and FF of devices fabricated using the  $\text{NH}_4\text{Cl}$  additive result from a highly crystalline, more uniform and smoother  $\text{CH}_3\text{NH}_3\text{PbI}_3$  film. The thickness of the  $\text{PC}_{61}\text{BM}$  layer was optimized (Table S3†). A 32 nm  $\text{PC}_{61}\text{BM}$  layer gave the best performance. A thinner  $\text{PC}_{61}\text{BM}$  layer can reduce the series resistance ( $R_s$ ) of devices, leading to higher FF. The FF decreased when further reducing the thickness of the  $\text{PC}_{61}\text{BM}$  layer, which resulted from the decrease of the shunt resistance. The solar cells fabricated using additives showed high reproducibility, which benefits from high crystallinity and good morphology of the  $\text{CH}_3\text{NH}_3\text{PbI}_3$  film. The integrated photocurrent for the devices fabricated using  $\text{CH}_3\text{NH}_3\text{Cl}$  and  $\text{NH}_4\text{Cl}$  additives is  $12.26 \text{ mA cm}^{-2}$  and  $13.32 \text{ mA cm}^{-2}$ , respectively, which is consistent with  $J_{sc}$  values obtained from  $J$ - $V$  measurements. The mechanism how  $\text{NH}_4\text{Cl}$  makes the perovskite film smooth is not clear, possibly related to crystallization kinetics.  $\text{NH}_4\text{Cl}$  could slow down the crystallization process to make perfect perovskite crystals. Good crystallinity and morphology for the perovskite layer favor exciton generation and charge carrier transport. Also, using a high-quality perovskite film, the above electron-transport layer can be made thinner to reduce the series resistance.

In summary, an innovative approach by using the chloride additive to enhance the performance of perovskite solar cells was developed. The effects of two additives  $\text{CH}_3\text{NH}_3\text{Cl}$  and

NH<sub>4</sub>Cl on perovskite film properties and photovoltaic performance were investigated. Perovskite films fabricated using the NH<sub>4</sub>Cl additive are highly crystalline and possess excellent morphology, leading to remarkable enhancement in the device performance. CH<sub>3</sub>NH<sub>3</sub>PbI<sub>3</sub>/PC<sub>61</sub>BM solar cells fabricated using the NH<sub>4</sub>Cl additive gave a decent PCE of 9.93% and a very outstanding FF of 80.11%. Application of this innovative approach in other device structures is ongoing in our lab.

## Acknowledgements

This work was supported by the “100 Talents Program” of Chinese Academy of Sciences and National Natural Science Foundation of China (21374025).

## Notes and references

- 1 M. M. Lee, J. Teuscher, T. Miyasaka, T. N. Murakami and H. J. Snaith, *Science*, 2012, **338**, 643.
- 2 H.-S. Kim, C.-R. Lee, J.-H. Im, K.-B. Lee, T. Moehl, A. Marchioro, S.-J. Moon, R. Humphry-Baker, J.-H. Yum, J. E. Moser, M. Grätzel and N.-G. Park, *Sci. Rep.*, 2012, **2**, 1.
- 3 J. Burschka, N. Pellet, S.-J. Moon, R. Humphry-Baker, P. Gao, M. K. Nazeeruddin and M. Grätzel, *Nature*, 2013, **499**, 316.
- 4 M. Liu, M. B. Johnston and H. J. Snaith, *Nature*, 2013, **501**, 395.
- 5 A. Kojima, K. Teshima, Y. Shirai and T. Miyasaka, *J. Am. Chem. Soc.*, 2009, **131**, 6050.
- 6 J.-H. Im, C.-R. Lee, J.-W. Lee, S.-W. Park and N.-G. Park, *Nanoscale*, 2011, **3**, 4088.
- 7 K. Wojciechowski, M. Saliba, T. Leijtens, A. Abate and H. J. Snaith, *Energy Environ. Sci.*, 2014, **7**, 1142.
- 8 S. Kazim, M. K. Nazeeruddin, M. Grätzel and S. Ahmad, *Angew. Chem., Int. Ed.*, 2014, **53**, 2812.
- 9 S. D. Stranks, G. E. Eperon, G. Grancini, C. Menelaou, M. J. P. Alcocer, T. Leijtens, L. M. Herz, A. Petrozza and H. J. Snaith, *Science*, 2013, **342**, 341.
- 10 J. H. Heo, S. H. Im, J. H. Noh, T. N. Mandal, C.-S. Lim, J. A. Chang, Y. H. Lee, H.-J. Kim, A. Sarkar, M. K. Nazeeruddin, M. Grätzel and S. I. Seok, *Nat. Photonics*, 2013, **7**, 486.
- 11 C. Roldán-Carmona, O. Malinkiewicz, A. Soriano, G. M. Espallargas, A. Garcia, P. Reinecke, T. Kroyer, M. I. Dar, M. K. Nazeeruddin and H. J. Bolink, *Energy Environ. Sci.*, 2014, **7**, 994.
- 12 J.-Y. Jeng, Y.-F. Chiang, M.-H. Lee, S.-R. Peng, T.-F. Guo, P. Chen and T.-C. Wen, *Adv. Mater.*, 2013, **25**, 3727.
- 13 S. Sun, T. Salim, N. Mathews, M. Duchamp, C. Boothroyd, G. Xing, T. C. Sum and Y. M. Lam, *Energy Environ. Sci.*, 2014, **7**, 399.
- 14 P. Docampo, J. M. Ball, M. Darwich, G. E. Eperon and H. J. Snaith, *Nat. Commun.*, 2013, **4**, 2761.
- 15 O. Malinkiewicz, A. Yella, Y. H. Lee, G. M. Espallargas, M. Grätzel, M. K. Nazeeruddin and H. J. Bolink, *Nat. Photonics*, 2014, **8**, 128.
- 16 H.-B. Kim, H. Choi, J. Jeong, S. Kim, B. Walker, S. Song and J. Y. Kim, *Nanoscale*, 2014, **6**, 6679.
- 17 G. E. Eperon, V. M. Burlakov, P. Docampo, A. Goriely and H. J. Snaith, *Adv. Funct. Mater.*, 2014, **24**, 151.
- 18 G. Xing, N. Mathews, S. Sun, S. S. Lim, Y. M. Lam, M. Grätzel, S. Mhaisalkar and T. C. Sum, *Science*, 2013, **342**, 344.
- 19 Q. Wang, Q. Dong, Z. Xiao, Y. Yuan and J. Huang, *Energy Environ. Sci.*, 2014, **7**, 2359.